

**Leptonic  $CP$  violation studies at MiniBooNE in the  $(3 + 2)$  sterile neutrino oscillation hypothesis**

G. Karagiorgi,<sup>\*</sup> A. Aguilar-Arevalo,<sup>†</sup> J.M. Conrad,<sup>‡</sup> and M.H. Shaevitz<sup>§</sup>  
*Department of Physics, Columbia University, New York, New York 10027, USA*

K. Whisnant<sup>||</sup>

*Department of Physics and Astronomy, Iowa State University, Ames, Iowa 50011, USA*

M. Sorel<sup>¶</sup>

*Instituto de Física Corpuscular, IFIC, CSIC and Universidad de Valencia, Spain*

V. Barger<sup>\*\*</sup>

*Department of Physics, University of Wisconsin, Madison, Wisconsin 53715, USA*  
 (Received 3 October 2006; published 29 January 2007)

We investigate the extent to which leptonic  $CP$ -violation in  $(3 + 2)$  sterile neutrino models leads to different oscillation probabilities for  $\bar{\nu}_\mu \rightarrow \bar{\nu}_e$  and  $\nu_\mu \rightarrow \nu_e$  oscillations at MiniBooNE. We are using a combined analysis of short-baseline (SBL) oscillation results, including the LSND and null SBL results, to which we impose additional constraints from atmospheric oscillation data. We obtain the favored regions in MiniBooNE oscillation probability space for both  $(3 + 2)$   $CP$ -conserving and  $(3 + 2)$   $CP$ -violating models. We further investigate the allowed  $CP$ -violation phase values and the MiniBooNE reach for such a  $CP$  violation measurement. The analysis shows that the oscillation probabilities in MiniBooNE neutrino and antineutrino running modes can differ significantly, with the latter possibly being as much as 3 times larger than the first. In addition, we also show that all possible values of the single  $CP$ -violation phase measurable at short baselines in  $(3 + 2)$  models are allowed within 99% CL by existing data.

DOI: [10.1103/PhysRevD.75.013011](https://doi.org/10.1103/PhysRevD.75.013011)

PACS numbers: 14.60.Pq, 14.60.St, 12.15.Ff

## I. INTRODUCTION

One of the most pressing open questions in neutrino physics today is whether or not leptons conserve the fundamental  $CP$  symmetry. The consequences of leptonic  $CP$  symmetry violation would be far-reaching and extend beyond the realm of particle physics, possibly being related to the matter-antimatter asymmetry observed in the Universe today [1].

In the standard paradigm of three-active-neutrino mixing occurring at the solar [2–8] and atmospheric [9–14] oscillation scales only, leptonic  $CP$  violation would yield different vacuum oscillation probabilities for neutrinos and antineutrinos that could be observed, for example, with accelerator-based neutrino oscillation appearance experiments operating near the atmospheric oscillation maximum [15,16]. This is because  $CP$ -odd terms in the oscillation probability formula would appear from solar/atmospheric interference terms involving the single  $CP$ -violating Dirac phase appearing in the neutrino mixing matrix [17].

Neutrino models involving active/sterile neutrino mixing [18] at the LSND [19] neutrino mass splitting scale via at least two sterile neutrino states [20,21] would open the possibility for further manifestations of leptonic  $CP$  violation, including ones that could be measurable with neutrino appearance experiments at short baselines also. In this paper, we investigate short-baseline (SBL) leptonic  $CP$ -violation in  $(3 + 2)$  sterile neutrino models. A schematic diagram describing  $(3 + 2)$  sterile neutrino models is shown in Fig. 1.

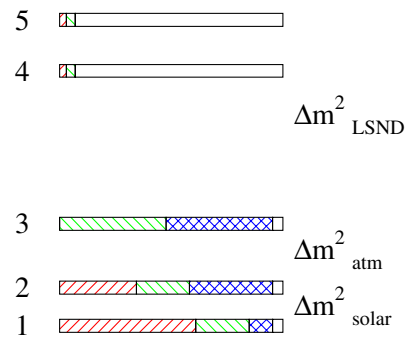


FIG. 1 (color online). Flavor content of neutrino mass eigenstates in  $(3 + 2)$  models. Neutrino masses increase from bottom to top. The  $\nu_e$  fractions are indicated by red (right-leaning) hatches, the  $\nu_\mu$  fractions by green (left-leaning) hatches, the  $\nu_\tau$  fractions by blue crosshatches, and the  $\nu_s$  fractions by no hatches. The flavor contents shown are schematic only [21].

<sup>\*</sup>Electronic address: georgia@nevis.columbia.edu

<sup>†</sup>Electronic address: alexis@phys.columbia.edu

<sup>‡</sup>Electronic address: conrad@nevis.columbia.edu

<sup>§</sup>Electronic address: shaevitz@nevis.columbia.edu

<sup>||</sup>Electronic address: whisnant@iastate.edu

<sup>¶</sup>Electronic address: sorel@ific.uv.es

<sup>\*\*</sup>Electronic address: barger@physics.wisc.edu

The analysis uses the same seven SBL datasets as in Ref. [21], including results on  $\nu_\mu$  disappearance (from the CCFR84 [22] and CDHS [23] experiments),  $\nu_e$  disappearance (from the Bugey [24] and CHOOZ [25] experiments), and  $\nu_\mu \rightarrow \nu_e$  oscillations (from the LSND [19], KARMEN2 [26], and NOMAD [27] experiments). In addition, additional atmospheric constraints have been added to the combined fit, based on the analysis of Ref. [28].

Based on the combined analysis of the above SBL and atmospheric oscillation data, we estimate the range of fundamental neutrino parameters in  $(3+2)$  sterile neutrino models that are allowed within the experimental capabilities of MiniBooNE, following a similar analysis to that in Ref. [21]. However, in this case, the  $CP$  conservation requirement is relaxed, allowing for different neutrino and antineutrino oscillation probabilities.

The paper is organized as follows. In Sec. II, we specify the neutrino oscillation formalism used in this analysis to describe  $(3+2)$ ,  $CP$ -violating neutrino oscillations. In Sec. III, we discuss the analysis followed in this paper, used to constrain neutrino oscillation parameters with short-baseline and atmospheric data. In Sec. IV, we present the results obtained for the  $CP$ -conserving, and  $CP$ -violating  $(3+2)$  models. For both cases, we explore the oscillation probability asymmetry experimentally allowed in MiniBooNE, and we quote the neutrino mass and mixing parameters for the best-fit models derived from the combined SBL + atmospheric constraint analysis. In Sec. V, we discuss the constraints on the single  $CP$ -violation phase that could be measured at short baselines, inferred from a  $CP$ -violating  $(3+2)$  analysis of SBL + atmospheric oscillation results, and how the MiniBooNE  $CP$  asymmetry observable is expected to vary as a function of this  $CP$ -violation phase.

## II. INCLUDING $CP$ VIOLATION IN THE STERILE NEUTRINO OSCILLATION FORMALISM

In the sterile neutrino oscillation formalism, under the assumptions of  $CPT$  invariance, the probability for a neutrino produced with flavor  $\alpha$  and energy  $E$ , to be detected as a neutrino of flavor  $\beta$  after traveling a distance  $L$ , is [29,30]:

$$P(\nu_\alpha \rightarrow \nu_\beta) = \delta_{\alpha\beta} - 4 \sum_{i>j} \mathcal{R}(U_{\alpha i}^* U_{\beta i} U_{\alpha j} U_{\beta j}^*) \sin^2 x_{ij} + 2 \sum_{i>j} \mathcal{I}(U_{\alpha i}^* U_{\beta i} U_{\alpha j} U_{\beta j}^*) \sin 2x_{ij} \quad (1)$$

where  $\mathcal{R}$  and  $\mathcal{I}$  indicate the real and imaginary parts of the product of mixing matrix elements, respectively;  $\alpha, \beta \equiv e, \mu, \tau$ , or  $s$ , ( $s$  being the sterile flavor);  $i, j = 1, \dots, N$  ( $N$  being the number of neutrino species); and  $x_{ij} \equiv 1.27 \Delta m_{ij}^2 L/E$ . In defining  $x_{ij}$ , we take the neutrino mass splitting  $\Delta m_{ij}^2 \equiv m_i^2 - m_j^2$  in  $\text{eV}^2$ , the neutrino baseline  $L$  in km, and the neutrino energy  $E$  in GeV. For antineutrinos,

the oscillation probability is obtained from Eq. (1) by replacing the mixing matrix  $U$  with its complex-conjugate matrix. Therefore, if the mixing matrix is not real, neutrino and antineutrino oscillation probabilities can differ.

For  $N$  neutrino species, there are, in general,  $(N-1)$  independent mass splittings,  $N(N-1)/2$  independent moduli of parameters in the unitary mixing matrix, and  $(N-1)(N-2)/2$  Dirac  $CP$ -violating phases that may be observed in oscillations.

In SBL neutrino experiments that are sensitive only to  $\nu_\mu \rightarrow \nu_\mu$ ,  $\nu_e \rightarrow \nu_e$ , and  $\nu_\mu \rightarrow \nu_e$  transitions, the set of observable parameters is reduced considerably. Firstly, oscillations due to atmospheric and solar mass splittings can be neglected in this case, or equivalently one can set  $m_1 = m_2 = m_3$ . Secondly, mixing matrix elements that measure the  $\tau$  neutrino flavor fraction of the various neutrino mass eigenstates do not enter in the oscillation probability. In this case, the number of observable parameters is restricted to  $(N-3)$  independent mass splittings,  $2(N-3)$  moduli of mixing matrix parameters, and  $N-4$   $CP$ -violating phases. Therefore, for  $(3+2)$  sterile neutrino models depicted in Fig. 1, that is for the  $N=5$  case, there are two independent mass splittings  $\Delta m_{41}^2$  and  $\Delta m_{51}^2$ , four moduli of mixing matrix parameters  $|U_{e4}|$ ,  $|U_{\mu 4}|$ ,  $|U_{e5}|$ ,  $|U_{\mu 5}|$ , and one  $CP$ -violating phase. The convention used in the following for this  $CP$ -phase is:

$$\phi_{45} = \arg(U_{\mu 5}^* U_{e5} U_{\mu 4} U_{e4}^*) \quad (2)$$

Under these assumptions, the general oscillation formula in Eq. (1) can be rewritten as:

$$P(\nu_\alpha \rightarrow \nu_\alpha) = 1 - 4[(1 - |U_{\alpha 4}|^2 - |U_{\alpha 5}|^2) \cdot (|U_{\alpha 4}|^2 \sin^2 x_{41} + |U_{\alpha 5}|^2 \sin^2 x_{51}) + |U_{\alpha 4}|^2 |U_{\alpha 5}|^2 \sin^2 x_{54}] \quad (3)$$

and

$$P(\nu_\mu \rightarrow \nu_e) = 4|U_{\mu 4}|^2 |U_{e4}|^2 \sin^2 x_{41} + 4|U_{\mu 5}|^2 |U_{e5}|^2 \sin^2 x_{51} + 8|U_{\mu 5}| |U_{e5}| |U_{\mu 4}| |U_{e4}| \sin x_{41} \sin x_{51} \times \cos(x_{54} + \phi_{45}) \quad (4)$$

The formulas for antineutrino oscillations are obtained by substituting  $\phi_{45} \rightarrow -\phi_{45}$ .

## III. ANALYSIS METHOD

The analysis we perform is a combined SBL + atmospheric analysis, with the purpose of obtaining the  $(3+2)$  model allowed regions in oscillation probability space for neutrino and antineutrino running modes expected at MiniBooNE, and the allowed values of the  $CP$ -violation phase  $\phi_{45}$ . The physics and statistical assumptions used in the analysis to describe the SBL experiments closely follow the ones described in detail in Ref. [21]. The Monte Carlo method used to apply the oscillation formalism discussed in Sec. II also closely follows the one described in Ref. [21]. The full set of

oscillation parameters  $(\Delta m_{41}^2, |U_{e4}|, |U_{\mu 4}|, \Delta m_{51}^2, |U_{e5}|, |U_{\mu 5}|, \phi_{45})$  is allowed to freely vary, constrained only by: (i)  $0.1 \text{ eV}^2 < \Delta m_{41}^2$ ,  $\Delta m_{51}^2 < 100 \text{ eV}^2$ , with  $\Delta m_{51}^2 \geq \Delta m_{41}^2$ , for definiteness; and (ii)  $|U_{ei}|^2 + |U_{\mu i}|^2 \leq 0.5$ , and  $|U_{\alpha 4}|^2 + |U_{\alpha 5}|^2 \leq 0.5$ . The first constraint defines the higher  $\Delta m^2$  splitting range considered, imposed by the LSND signature, whereas the second constraint requires the fourth and fifth mass eigenstates to include only small active flavor quantities, as suggested by the solar and atmospheric oscillation data.

A slight modification was made to the analysis method used in this paper, compared to the one used in Ref. [21]. Rather than generating neutrino masses and mixings in a random, unbiased way, we use importance sampling via a Markov chain Monte Carlo method [31,32], to better sample the regions in parameter space that provide a good fit to the SBL + atmospheric data. Given a starting point (model)  $x_i$  in the  $(\Delta m_{41}^2, |U_{e4}|, |U_{\mu 4}|, \Delta m_{51}^2, |U_{e5}|, |U_{\mu 5}|, \phi_{45})$  parameter space, a trial state  $x_{i+1} = x_i + e$  that depends only on the current state  $x_i$  and on the probability distribution function for the random vector  $e$ , is generated. The probability for the trial state  $x_{i+1}$  to be accepted as the new current state for further model random generation is given by the transition probability:

$$P(x_i \rightarrow x_{i+1}) = \min\{1, \exp[-(\chi_{i+1}^2 - \chi_i^2)/T]\} \quad (5)$$

where  $\chi_i^2$  and  $\chi_{i+1}^2$  are  $\chi^2$  values for the states  $x_i$  and  $x_{i+1}$ , quantifying the agreement between the models and the short-baseline plus atmospheric results used in the combined analysis, and  $T$  is an effective ‘‘temperature’’ parameter. The results presented here are obtained by combining various Markov chains with different initial conditions, probability distribution functions for  $e$ , and temperature parameters. This modification allows for an efficient probe of the larger dimensionality of the parameter set present in  $CP$ -violating models, compared to  $CP$ -conserving models.

The addition of atmospheric constraints to our previous analysis [21] follows the assumptions discussed in Ref. [28]. These constraints include 1489 days of Super-Kamiokande charged-current data [9], including the  $e$ -like and  $\mu$ -like data samples of sub- and multi-GeV contained events, stopping events, and through-going upgoing muon data events. The analysis in Ref. [28] assumes the three-dimensional atmospheric neutrino fluxes given in [33], and a treatment of flux, cross-section, and experimental systematic uncertainties given in [34]. The atmospheric constraint includes also data on  $\nu_\mu$  disappearance from the long baseline, accelerator-based experiment K2K [13]. The atmospheric constraint is implemented in our analysis by simply adding a contribution  $\chi_{\text{atm}}^2 = \chi_{\text{atm}}^2(d_\mu)$  to the total SBL contribution,  $\chi_{\text{SBL}}^2 = \chi_{\text{SBL}}^2(\Delta m_{41}^2, |U_{e4}|, |U_{\mu 4}|, \Delta m_{51}^2, |U_{e5}|, |U_{\mu 5}|, \phi_{45})$ , where:

$$d_\mu = \frac{1 - \sqrt{1 - 4A}}{2} \quad (6)$$

with:

$$A \equiv (1 - |U_{\mu 4}|^2 - |U_{\mu 5}|^2)(|U_{\mu 4}|^2 + |U_{\mu 5}|^2) + |U_{\mu 4}|^2 |U_{\mu 5}|^2 \quad (7)$$

and by consequently adding a single degree of freedom to our analysis. We note that the recent analysis of atmospheric + K2K data in Ref. [28] constrain the quantity  $d_\mu$  in Eq. (6), and therefore muon neutrino disappearance at the LSND mass splitting scale, significantly more than previous results. For reference, the authors of Ref. [28] quote an upper limit on  $d_\mu$  of 0.065 at 99% C.L., while  $d_\mu \leq 0.13$  at 99% C.L. is given in Ref. [35].

The combined  $\chi^2$  used to extract the best-fit values and allowed ranges for the fundamental oscillation parameters  $\Delta m_{41}^2, \Delta m_{51}^2, U_{e4}, U_{\mu 4}, U_{e5}, U_{\mu 5}$ , given in Secs. IV and V, is therefore:

$$\chi^2 \equiv \chi_{\text{SBL}}^2 + \chi_{\text{atm}}^2 \quad (8)$$

In  $CP$ -conserving models,  $\phi_{45}$  is only allowed to take values of 0, or  $\pi$ , whereas in  $CP$ -violating models,  $\phi_{45}$  can vary within the full  $(0, 2\pi)$  range. Inclusion of this additional parameter reduces the total number of degrees of freedom by one.

This analysis also provides realistic estimates of the oscillation probabilities to be expected in MiniBooNE in the framework of allowed  $CP$ -conserving and  $CP$ -violating  $(3 + 2)$  sterile neutrino models. For that, expected neutrino transmutation rates for full  $\nu_\mu \rightarrow \nu_e$  or  $\bar{\nu}_\mu \rightarrow \bar{\nu}_e$  transmutations as a function of neutrino or antineutrino energy are considered, for neutrino and antineutrino running modes in MiniBooNE. These distributions are weighted according to the oscillation probability formula in Eq. (4) to estimate the number of oscillation signal events for any  $(3 + 2)$  model, prior to event reconstruction and particle identification. The predictions for the full-transmutation rates are obtained by multiplying the flux distributions as a function of energy for muon neutrinos and antineutrinos in both neutrino and antineutrino running modes (four flux distributions in total) by the (energy-dependent) total electron neutrino and antineutrino cross-sections on  $\text{CH}_2$ , respectively. The flux predictions are obtained from a full simulation of the FNAL Booster neutrino beamline [36], while the neutrino cross-section predictions are obtained from the NUANCE event generator [37]. We do, therefore, take into account also the effect of ‘‘wrong sign’’ neutrinos in computing the expected oscillation probabilities, which have the effect of washing out  $CP$ -violating observables. This effect is non-negligible since as much as one third of the total interaction rate in antineutrino running mode is expected to be due to neutrinos rather than antineutrinos; on the other hand, the

antineutrino contribution in neutrino running mode is expected to be much smaller.

#### IV. OSCILLATION PROBABILITY EXPECTATIONS FOR MINIBOOONE

We define the oscillation probability in neutrino (antineutrino) mode expected at MiniBooNE as:

$$\bar{p}_{\text{BooNE}}^{(-)} = \frac{\int dE [p(\nu_\mu \rightarrow \nu_e) \bar{N}_0(\nu) + p(\bar{\nu}_\mu \rightarrow \bar{\nu}_e) \bar{N}_0(\bar{\nu})]}{\int dE [\bar{N}_0(\nu) + \bar{N}_0(\bar{\nu})]} \quad (9)$$

where  $E$  is the neutrino energy;  $p(\nu_\mu \rightarrow \nu_e)$  and  $p(\nu_{\bar{\mu}} \rightarrow \nu_{\bar{e}})$  are the oscillation probabilities given by Eq. (4), with  $\phi_{45} = 0$  or  $\pi$  for the  $CP$ -conserving case, and  $0 < \phi_{45} < 2\pi$  for the  $CP$ -violating case;  $N_0(\nu)$  and  $N_0(\bar{\nu})$  are the MiniBooNE neutrino and antineutrino full-transmutation rate distributions in neutrino running mode, and  $\bar{N}_0(\nu)$  and  $\bar{N}_0(\bar{\nu})$  are the neutrino and antineutrino full-transmutation rate distributions in antineutrino running mode, as defined in Sec. III.

This section consists of two parts. In the first part, we explore the experimentally allowed asymmetry in neutrino and antineutrino mode oscillation probabilities,  $A_{p/\bar{p}}$ , obtained from the SBL + atmospheric analysis assuming  $(3 + 2)$   $CP$ -conserving models, as a function of the average oscillation probability allowed,  $\langle p_{\text{BooNE}} \rangle$ . The asymmetry in oscillation probabilities and the average oscillation probability are defined in Eq. (10) and (11), respectively.

$$A_{p/\bar{p}} = \frac{p_{\text{BooNE}} - \bar{p}_{\text{BooNE}}}{p_{\text{BooNE}} + \bar{p}_{\text{BooNE}}} \quad (10)$$

$$\langle p_{\text{BooNE}} \rangle = (p_{\text{BooNE}} + \bar{p}_{\text{BooNE}})/2 \quad (11)$$

In the second part, we explore the allowed oscillation probability space  $(p_{\text{BooNE}}, \bar{p}_{\text{BooNE}})$  for  $(3 + 2)$   $CP$ -violating models. In both parts, we quote the values for the masses and mixing parameters corresponding to the best-fit models in the  $(p_{\text{BooNE}}, \bar{p}_{\text{BooNE}})$  space.

The 90%, and 99% CL allowed region are defined as the  $(A_{p/\bar{p}}, \langle p_{\text{BooNE}} \rangle)$  or  $(p_{\text{BooNE}}, \bar{p}_{\text{BooNE}})$  space for which  $\chi^2 - \chi_{\text{min}}^2 < 4.61$ , and  $\chi^2 - \chi_{\text{min}}^2 < 9.21$ , respectively, where  $\chi_{\text{min}}^2$  is the absolute  $\chi^2$  minimum for all  $(p_{\text{BooNE}}, \bar{p}_{\text{BooNE}})$  values.

##### A. $CP$ -conserving models results

Figure 2 shows predictions for the asymmetry in oscillation probabilities expected in MiniBooNE neutrino and antineutrino modes, in the  $CP$ -conserving,  $(3 + 2)$  sterile neutrino hypothesis. The bottom panel in Fig. 2 shows the region in  $(A_{p/\bar{p}}, \langle p_{\text{BooNE}} \rangle)$  space that is allowed at the 90% and 99% confidence level (2 dof) by existing short-

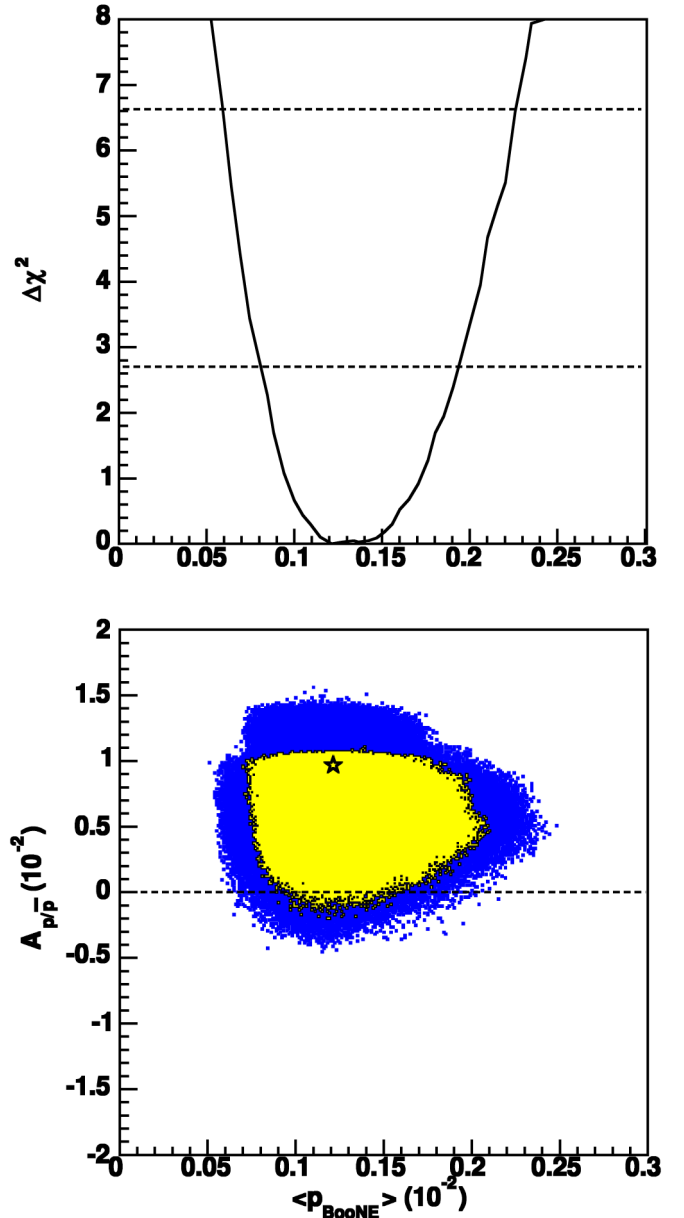


FIG. 2 (color online). Expected oscillation probability asymmetry at MiniBooNE for neutrino and antineutrino running modes, for  $CP$ -conserving  $(3 + 2)$  models. The yellow (light gray) region corresponds to the 90% CL allowed region; the blue (dark gray) region corresponds to the 99% CL allowed region. See text for details.

TABLE I. Comparison of best-fit values for mass-splittings and mixing parameters for  $(3 + 2)$   $CP$ -conserving and  $CP$ -violating models. Mass splittings are shown in  $\text{eV}^2$ . See text for details.

Model	$\chi^2(\text{d.o.f.})$	$\Delta m_{41}^2$	$\Delta m_{51}^2$	$ U_{e4} $	$ U_{\mu 4} $	$ U_{e5} $	$ U_{\mu 5} $	$\phi_{45}$
CPC	141.4 (145)	0.92	24	0.132	0.158	0.066	0.159	0
CPV	140.8 (144)	0.91	24	0.127	0.147	0.068	0.164	$1.8\pi$

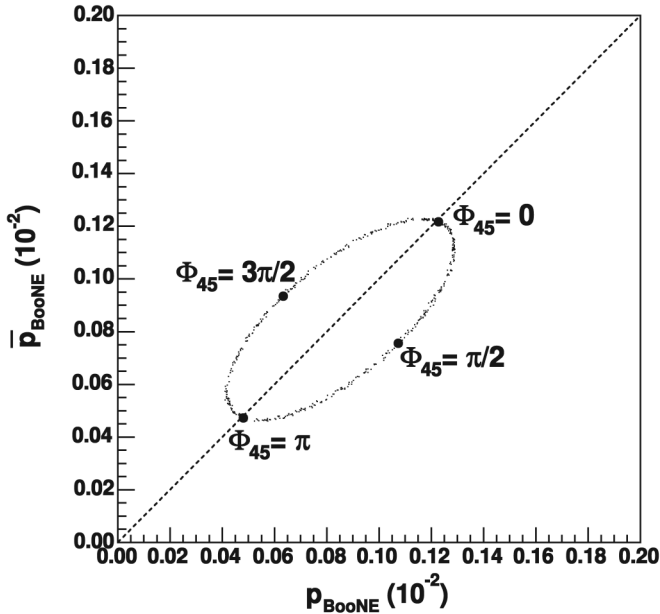


FIG. 3. Illustration of expected oscillation probabilities at MiniBooNE in neutrino and antineutrino running modes, for  $CP$ -violating  $(3+2)$  models with atmospheric constraint. Here, the neutrino masses and mixings are fixed to their best-fit values and the only parameter that is allowed to vary is the  $CP$ -violating phase,  $\phi_{45}$ .

baseline data used in the analysis, including LSND. The star indicates the best-fit, at  $p_{\text{BooNE}} \approx \bar{p}_{\text{BooNE}} \approx 0.13 \cdot 10^{-2}$ . The effect of “fake”  $CP$ -violation due to spectrum differences in neutrino and antineutrino running modes manifests itself as a departure from zero-asymmetry indicated by the dotted line in the bottom panel of Fig. 2. The effect is at the percent level at most.

The top panel in Fig. 2 shows the 1-dimensional projection of the  $\Delta\chi^2$  contour obtained from the SBL+atmospheric data, as a function of average oscillation probability  $\langle p_{\text{BooNE}} \rangle$ . The dashed lines at  $\Delta\chi^2 = 2.70$  and  $6.63$  indicate the 90% and 99% CL regions, respectively, (1 dof). MiniBooNE is expected to measure an oscillation probability in excess of  $\approx 0.05 \cdot 10^{-2}$  if  $CP$ -conserving  $(3+2)$  models are correct.

The best-fit model parameters for  $CP$ -conserving  $(3+2)$  sterile neutrino oscillation models are shown in Table I.

### B. $CP$ -violating models results

Figure 3 shows the order of magnitude of the  $CP$ -violating effects to be expected in  $(p_{\text{BooNE}}, \bar{p}_{\text{BooNE}})$  space, as  $\phi_{45}$  is varied over its allowed range  $(0, 2\pi)$ , while the remaining oscillation parameters are fixed to their best-fit values for the  $CP$ -conserving case. In this particular Figure, where we neglect goodness-of-fit considerations of

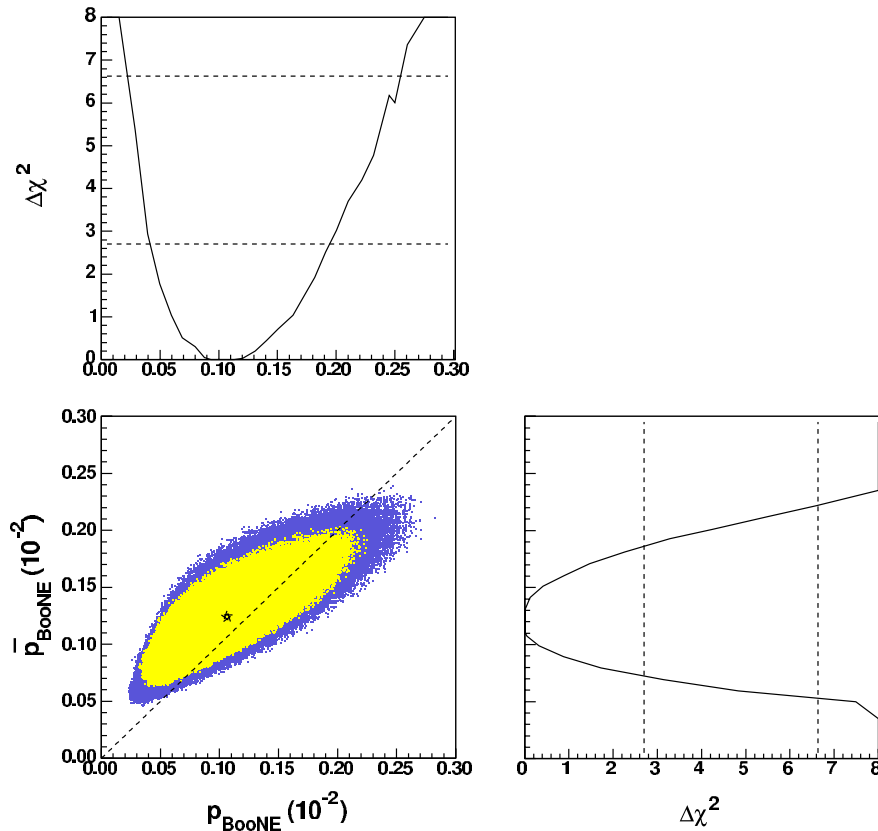


FIG. 4 (color online). Expected oscillation probabilities at MiniBooNE in neutrino and antineutrino running modes, for  $CP$ -violating  $(3+2)$  models. The yellow (light gray) region corresponds to the 90% CL allowed region; the blue (dark gray) region corresponds to the 99% CL allowed region. See text for details.

the SBL + atmospheric datasets as a function of  $\phi_{45}$  variations, neutrino/antineutrino oscillation probability differences as large as a factor of 2 can be obtained, near maximal  $CP$ -violation ( $\phi_{45} = \pi/2$  or  $3\pi/2$ ). As will be seen below, a similar conclusion (with actually even larger differences allowed among neutrino and antineutrino running modes) is reached with a more quantitative analysis that takes into account  $\chi^2$  variations as a function of all neutrino parameters.

Figure 4 shows the oscillation probabilities to be expected at MiniBooNE in neutrino and antineutrino running modes, in a  $CP$ -violating,  $(3+2)$  scenario. Unlike in Fig. 3, in Fig. 4 all parameters ( $\Delta m_{41}^2, \Delta m_{51}^2, |U_{e4}|, |U_{\mu 4}|, |U_{e5}|, |U_{\mu 5}|, \phi_{45}$ ) are now allowed to vary within the constraints provided by existing SBL + atmospheric oscillation results. Compared to the  $CP$ -conserving case of Fig. 2, the best-fit point (indicated by a star) does not change significantly; however, large asymmetries in oscillation probability due to  $CP$ -violation are now possible, shown by departures from the dashed line in the bottom left panel of Fig. 4. The general trend is that the 2-dimensional allowed region in  $(p_{\text{BooNE}}, \bar{p}_{\text{BooNE}})$  space is tilted more horizontally compared to the dashed line  $\bar{p}_{\text{BooNE}} = p_{\text{BooNE}}$ , indicating that existing short-

baseline results constrain more  $\bar{\nu}_\mu \rightarrow \bar{\nu}_e$  than  $\nu_\mu \rightarrow \nu_e$  oscillations.

The best-fit model parameters for  $CP$ -violating  $(3+2)$  sterile neutrino oscillation models are shown in Table I. From a comparison of the  $\chi^2$  values given in the Table, it is clear that  $CP$ -violating,  $(3+2)$  models do not provide a significantly better description of short-baseline and atmospheric data, compared to  $CP$ -conserving,  $(3+2)$  models.

## V. CONSTRAINTS ON $CP$ -VIOLATION PHASE

In this section we discuss the present constraints on the short-baseline,  $CP$ -violating phase  $\phi_{45}$  that the current SBL + atmospheric oscillation data impose on  $(3+2)$  sterile neutrino oscillation models, and the prospects of observing such phase at MiniBooNE. The top left panel in Fig. 5 shows that all values for the  $CP$ -phase  $\phi_{45}$  are presently allowed at the 99% confidence level, and that  $CP$ -violating,  $(3+2)$  models with small degrees of  $CP$  violation are marginally preferred. The bottom left plot shows that large  $CP$  asymmetry is possible, but not required, for maximal  $CP$ -violation, given by phases of around  $\phi_{45} = \pi/2$  and  $3\pi/2$ . In particular,  $CP$  asymme-

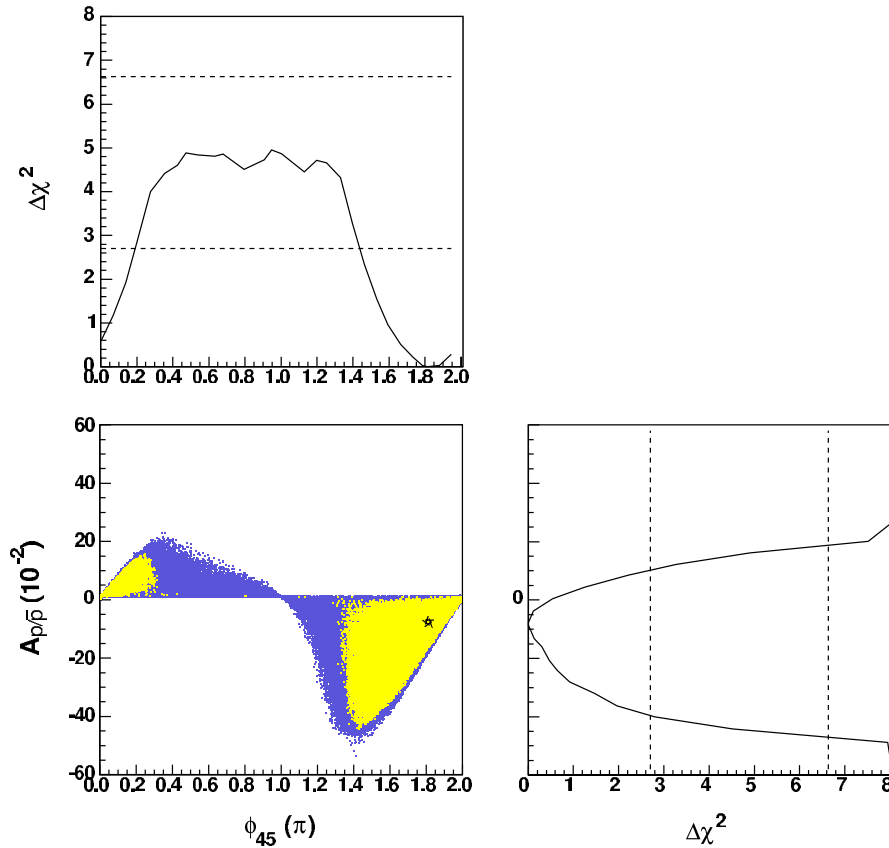


FIG. 5 (color online). Current limits on the  $CP$ -violating phase  $\phi_{45}$  from current short-baseline results, and  $CP$  asymmetry measurement expected at MiniBooNE,  $A_{p/\bar{p}}$ , as a function of  $\phi_{45}$ . The yellow (light gray) region corresponds to the 90% CL allowed region; the blue (dark gray) region corresponds to the 99% CL allowed region. See text for details.

tries up to  $A_{p/\bar{p}} \approx -0.5$  could be obtained, where  $A_{p/\bar{p}}$  is defined in Eq. (10). The value  $A_{p/\bar{p}} = -0.5$  corresponds to 3 times larger oscillation probability in antineutrino running mode, compared to the neutrino running mode probability. Comparing Fig. 5 with Fig. 2, we conclude that a significant departure from zero in the asymmetry observable  $A_{p/\bar{p}}$  could naturally be interpreted as a manifestation of leptonic  $CP$  violation.

## VI. CONCLUSIONS

We have performed a combined analysis of data from seven short-baseline experiments (Bugey, CHOOZ, CCFR84, CDHS, KARMEN, LSND, NOMAD), and including also constraints from atmospheric oscillation data (Super-Kamiokande, K2K), for the  $(3 + 2)$  neutrino oscillation hypothesis, with two sterile neutrinos at high  $\Delta m^2$ . The motivation for considering two light, sterile neutrino models arises from the tension in trying to reconcile, in a  $CPT$ -conserving framework, the LSND signal for oscillations with the null results obtained by the other SBL experiments with a single light sterile neutrino state [21,38–40]. The class of  $(3 + 2)$  sterile neutrino models open up the possibility of observing possible leptonic  $CP$ -violating effects at short-baseline experiments, and, in particular, within the experimental capabilities of MiniBooNE.

We have described two types of analyses in the  $(3 + 2)$  neutrino oscillation hypothesis. In the first analysis, we treat the SBL datasets with additional atmospheric constraints in a  $CP$ -conserving scenario, and we determine the allowed oscillation probabilities at MiniBooNE in both neutrino and antineutrino running modes, as well as the best-fit values for the mass splittings and mixing parameters. In the second analysis, we consider a  $CP$ -violating scenario to obtain the favored regions in MiniBooNE oscillation probability space, we determine the best-fit values for the mass splittings and mixing parameters, and we further investigate the allowed  $CP$ -violating phase

values, quoting the best-fit value for the  $CP$ -violating phase.

The main results of the analysis are given in Secs. IV and V. First, we find that  $CP$ -violating,  $(3 + 2)$  models do not provide a significantly better description of short-baseline and atmospheric data, compared to  $CP$ -conserving,  $(3 + 2)$  models. On the other hand, even if only a small degree of  $CP$  violation is marginally preferred, we also find that existing data allow for all possible values for the single  $CP$ -violating phase that could be observed at short baselines in  $(3 + 2)$  models, at 99% C.L.. Finally, if leptonic  $CP$  violation occurs and  $(3 + 2)$  sterile neutrino models are a good description of the data, we find that differences as large as a factor of 3 between the electron (anti-)neutrino appearance probabilities in neutrino and antineutrino running modes at MiniBooNE are possible.

The existence of a fifth neutrino with mass of order 5 eV, as found in our fits, would be in conflict with cosmological bounds obtained under the assumption that all the neutrinos are in thermal equilibrium, see, e.g., [41]. However, these bounds may be avoided if the neutrinos do not thermalize [42] or if the reheating temperature of the universe is very low [43].

## ACKNOWLEDGMENTS

We thank O. Yasuda for useful suggestions, M. Maltoni for providing the data on atmospheric constraints, the MiniBooNE Collaboration for providing the neutrino flux and cross-section expectations for the MiniBooNE experiment, K. Abazajian for introducing one of us (MS) to Markov chain Monte Carlo simulations, and S. Parke for enlightening discussions and for pointing out a mistake in an earlier version of this paper. This work was supported by NSF grant No. PHY-0500492, by U.S. Department of Energy grant Nos. DE-FG02-95ER40896 and DE-FG02-01ER41155, by the Wisconsin Alumni Research Foundation, and by the European Community grant No. MEIF-CT-2005-009487.

- 
- [1] A. D. Sakharov, *Pisma Zh. Eksp. Teor. Fiz.* **5**, 32 (1967); [*JETP Lett.* **5**, 24 (1967) SOPUA **34**, 392 (1991) UFNAA **161**, 61 (1991)].
  - [2] B. T. Cleveland *et al.*, *Astrophys. J.* **496**, 505 (1998).
  - [3] Y. Fukuda *et al.* (Super-Kamiokande Collaboration), *Phys. Rev. Lett.* **81**, 1158 (1998); **81**, 4279(E) (1998); **82**, 2430 (1999).
  - [4] J. N. Abdurashitov *et al.* (SAGE Collaboration), *J. Exp. Theor. Phys.* **95**, 181 (2002) [*Zh. Eksp. Teor. Fiz.* **122**, 211 (2002)].
  - [5] W. Hampel *et al.* (GALLEX Collaboration), *Phys. Lett. B* **447**, 127 (1999).
  - [6] M. Altmann *et al.* (GNO Collaboration), *Phys. Lett. B* **490**, 16 (2000).
  - [7] Q. R. Ahmad *et al.* (SNO Collaboration), *Phys. Rev. Lett.* **89**, 011301 (2002); **89**, 011302 (2002); **87**, 071301 (2001).
  - [8] T. Araki *et al.* (KamLAND Collaboration), *Phys. Rev. Lett.* **94**, 081801 (2005).
  - [9] Y. Fukuda *et al.* (Super-Kamiokande Collaboration), *Phys. Lett. B* **433**, 9 (1998); **436**, 33 (1998); *Phys. Rev. Lett.* **81**, 1562 (1998); **82**, 2644 (1999); *Phys. Lett. B* **467**, 185 (1999); Y. Ashie *et al.* (Super-Kamiokande Collaboration), *Phys. Rev. D* **71**, 112005 (2005).
  - [10] D. Casper *et al.*, *Phys. Rev. Lett.* **66**, 2561 (1991); R.

- Becker-Szendy *et al.*, Phys. Rev. Lett. **69**, 1010 (1992).
- [11] M. Ambrosio *et al.* (MACRO Collaboration), Phys. Lett. B **434**, 451 (1998); **478**, 5 (2000); **517**, 59 (2001); **566**, 35 (2003).
- [12] W. W. M. Allison *et al.*, Phys. Lett. B **391**, 491 (1997); **449**, 137 (1999); M. C. Sanchez *et al.* (Soudan 2 Collaboration), Phys. Rev. D **68**, 113004 (2003).
- [13] S. H. Ahn *et al.* (K2K Collaboration), Phys. Lett. B **511**, 178 (2001); Phys. Rev. Lett. **90**, 041801 (2003); Phys. Rev. D **74**, 072003 (2006).
- [14] D. G. Michael *et al.* (MINOS Collaboration), Phys. Rev. Lett. **97**, 191801 (2006).
- [15] V. Barger, D. Marfatia, and K. Whisnant, Int. J. Mod. Phys. E **12**, 569 (2003).
- [16] O. Mena, Mod. Phys. Lett. A **20**, 1 (2005).
- [17] V. Barger, K. Whisnant, and R. J. N. Phillips, Phys. Rev. Lett. **45**, 2084 (1980).
- [18] J. J. Gomez-Cadenas and M. C. Gonzalez-Garcia, Z. Phys. C **71**, 443 (1996).
- [19] C. Athanassopoulos *et al.* (LSND Collaboration), Phys. Rev. Lett. **77**, 3082 (1996); Phys. Rev. C **58**, 2489 (1998); A. Aguilar *et al.* (LSND Collaboration), Phys. Rev. D **64**, 112007 (2001).
- [20] O. L. G. Peres and A. Y. Smirnov, Nucl. Phys. **B599**, 3 (2001).
- [21] M. Sorel, J. M. Conrad, and M. H. Shaevitz, Phys. Rev. D **70**, 073004 (2004).
- [22] I. E. Stockdale *et al.*, Phys. Rev. Lett. **52**, 1384 (1984).
- [23] F. Dydak *et al.*, Phys. Lett. B **134**, 281 (1984).
- [24] Y. Declais *et al.*, Nucl. Phys. **B434**, 503 (1995).
- [25] M. Apollonio *et al.*, Eur. Phys. J. C **27**, 331 (2003).
- [26] B. Armbruster *et al.* (KARMEN Collaboration), Phys. Rev. D **65**, 112001 (2002).
- [27] P. Astier *et al.* (NOMAD Collaboration), Phys. Lett. B **570**, 19 (2003); D. Gibin, Nucl. Phys. B, Proc. Suppl. **66**, 366 (1998); V. Valuev (NOMAD Collaboration), International Europhysics Conference on High-Energy Physics (HEP 2001), Budapest, Hungary, 2001.
- [28] M. Maltoni, T. Schwetz, M. Tortola, and J. W. F. Valle, New J. Phys. **6**, 122 (2004).
- [29] V. Barger, Y. B. Dai, K. Whisnant, and B. L. Young, Phys. Rev. D **59**, 113010 (1999).
- [30] B. Kayser, hep-ph/0211134.
- [31] P. Brâemaud, *Markov Chains: Gibbs Fields, Monte Carlo Simulation, and Queues* (Springer, New York, 1999).
- [32] N. Metropolis, A. W. Rosenbluth, M. N. Rosenbluth, A. H. Teller, and E. Teller, J. Chem. Phys. **21**, 1087 (1953).
- [33] M. Honda, T. Kajita, K. Kasahara, and S. Midorikawa, Phys. Rev. D **70**, 043008 (2004).
- [34] M. C. Gonzalez-Garcia and M. Maltoni, Phys. Rev. D **70**, 033010 (2004).
- [35] M. Maltoni, T. Schwetz, and J. W. F. Valle, Phys. Lett. B **518**, 252 (2001).
- [36] A. A. Aguilar-Arevalo *et al.* (MiniBooNE Collaboration), "The MiniBooNE Run Plan", <http://www-boone.fnal.gov/publicpages/runplan.ps.gz>.
- [37] D. Casper, Nucl. Phys. B, Proc. Suppl. **112**, 161 (2002).
- [38] M. Maltoni, T. Schwetz, M. A. Tortola, and J. W. F. Valle, Nucl. Phys. **B643**, 321 (2002).
- [39] A. Strumia, Phys. Lett. B **539**, 91 (2002).
- [40] W. Grimus and T. Schwetz, Eur. Phys. J. C **20**, 1 (2001).
- [41] S. Hannestad, Prog. Part. Nucl. Phys. **57**, 309 (2006).
- [42] K. Abazajian, N. F. Bell, G. M. Fuller, and Y. Y. Y. Wong, Phys. Rev. D **72**, 063004 (2005).
- [43] G. Gelmini, S. Palomares-Ruiz, and S. Pascoli, Phys. Rev. Lett. **93**, 081302 (2004).